

Revealing Effects of Molecular-Orientation on Azo Coupling Reaction of Nitro Compounds Driven by Surface Plasmonic Resonances

Ying-Jen Shiu,^a Michitoshi Hayashi,^{b,*} and Ying-Huang Lai,^c U-Ser Jeng^{a,d,*}

a. National Synchrotron Radiation Research Center, Hsinchu 30076, Taiwan. E-mail: usjeng@nsrrc.org.tw

b. Center for Condensed Matter Sciences, National Taiwan University, Taipei, Taiwan. E-mail: atmyh@ntu.edu.tw

c. Department of Chemistry, Tunghai University, No. 1727, Sec. 4, Taiwan Boulevard, 40704, Taichung, Taiwan.

d. Chemical Engineering Department, National Tsing-Hua University, Hsinchu, 30013, Taiwan

*Corresponding authors

1. Configurations of the molecular models

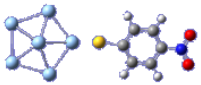
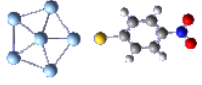
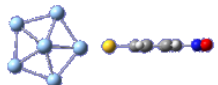
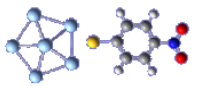
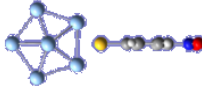
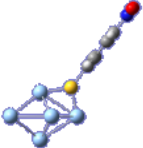
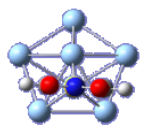
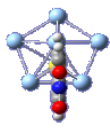
	i	ii		iii
I	 (1-1) ($\theta = 0^\circ$ vs $Ag(\overline{BC})$)	 (1-2) ($\theta = 45^\circ$ vs $Ag(\overline{BC})$)		-
II	 (2-1) ($\theta = 0^\circ$ vs $Ag(\overline{AG})$)	 (2-2) ($\theta = 45^\circ$ vs $Ag(\overline{AG})$)		 (2-3) ($\theta = 90^\circ$ vs $Ag(\overline{AG})$)
III	 (3-1) ($\theta = 90^\circ$ vs $Ag(\overline{AG})$)	 (3-2) ($\theta = 45^\circ$ vs $Ag(\overline{AG})$)		 (3-3) ($\theta = 0^\circ$ vs $Ag(\overline{AG})$)
IV	 (4-1) ($\theta = 0^\circ$ vs $Ag(\overline{AB})$)	 (4-2) ($\theta = 45^\circ$ vs $Ag(\overline{AB})$)		-
V	 (5-1) ($\theta = 0^\circ$ vs $Ag(\overline{BC})$)	 (5-2) ($\theta = 45^\circ$ vs $Ag(\overline{BC})$)		 (5-3) ($\theta = 90^\circ$ vs $Ag(\overline{BC})$)

Figure S1a. Thirteen initial structures classified with the five adsorption sites I – V indicated, and two or three related orientations (i, ii, and iii) between the reactant 4-NTP and the cluster Ag_7 (sky-blue balls). The angle θ is the inclined angle between the vector \vec{N} (the normal axis of phenyl ring) and the Ag bonds ($Ag(\overline{BC})$, $Ag(\overline{AG})$, and $Ag(\overline{AB})$), modulated by rotating 4NTP along C-S bond, shown in Figure S1b (reproduced from Figure 1 for convenience).

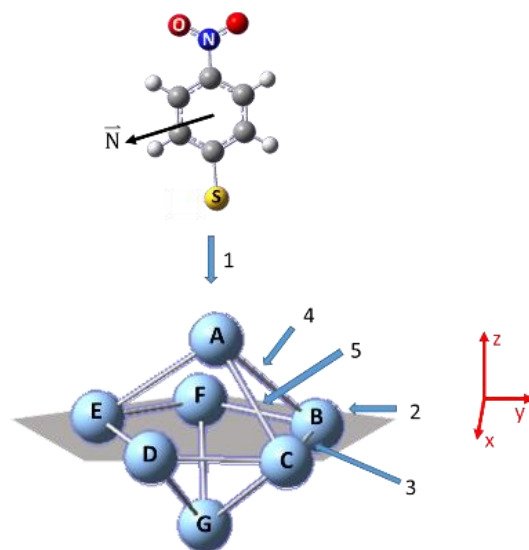


Figure S1b. Schematic illustration of the initial structure of 4NTP on the Ag_7 cluster, optimized with five possible adsorption sites (1 – 5 as indicated by the arrows). The grey pentagon formed with the Ag atoms B-E are defined as the x-y plane, and A and G are on the z-axis. \vec{N} defines the normal axis of the benzene ring.

Table S1. Parameters describing the related orientation of 4NTP vs. Ag_7 . the incline angles α and β formed by the normal axis of the phenyl ring (\vec{N}) with the pentagonal plan of Ag_7 and the triangular facet $\text{Ag}(\text{ABC})$ characterize conveniently the 4NTP molecular orientation (Figure S1).

	opt.(I)	opt.(O)	opt.(T)	opt.(M)	opt.(N)
S-Ag(A) (Å)	2.56	4.04	2.46	3.76	2.49
S-Ag(B) (Å)	3.85	2.69	4.86	2.74	4.05
S-Ag(C) (Å)	2.86	2.69	4.74	2.82	4.17
S-Ag(G) (Å)	4.92	4.76	5.55	4.89	5.43
$\angle \text{Ag}(\text{A}) - \text{S} - \text{Ag}(\text{B})$ (°)	48.4	45.5	26.8	49.6	45.0
$\angle \text{Ag}(\text{A}) - \text{S} - \text{Ag}(\text{C})$ (°)	64.0	45.5	30.1	49.4	42.6
$\angle \text{Ag}(\text{A}) - \text{S} - \text{Ag}(\text{G})$ (°)	33.0	40.2	4.4	39.3	15.3
$\angle \text{Ag}(\text{B}) - \text{S} - \text{Ag}(\text{C})$ (°)	47.6	64.2	34.6	61.7	41.0
α (°)	12.8	52.3	60.1	48.6	26.6
β (°)	50.4	14.1	62.2	27.2	43.5

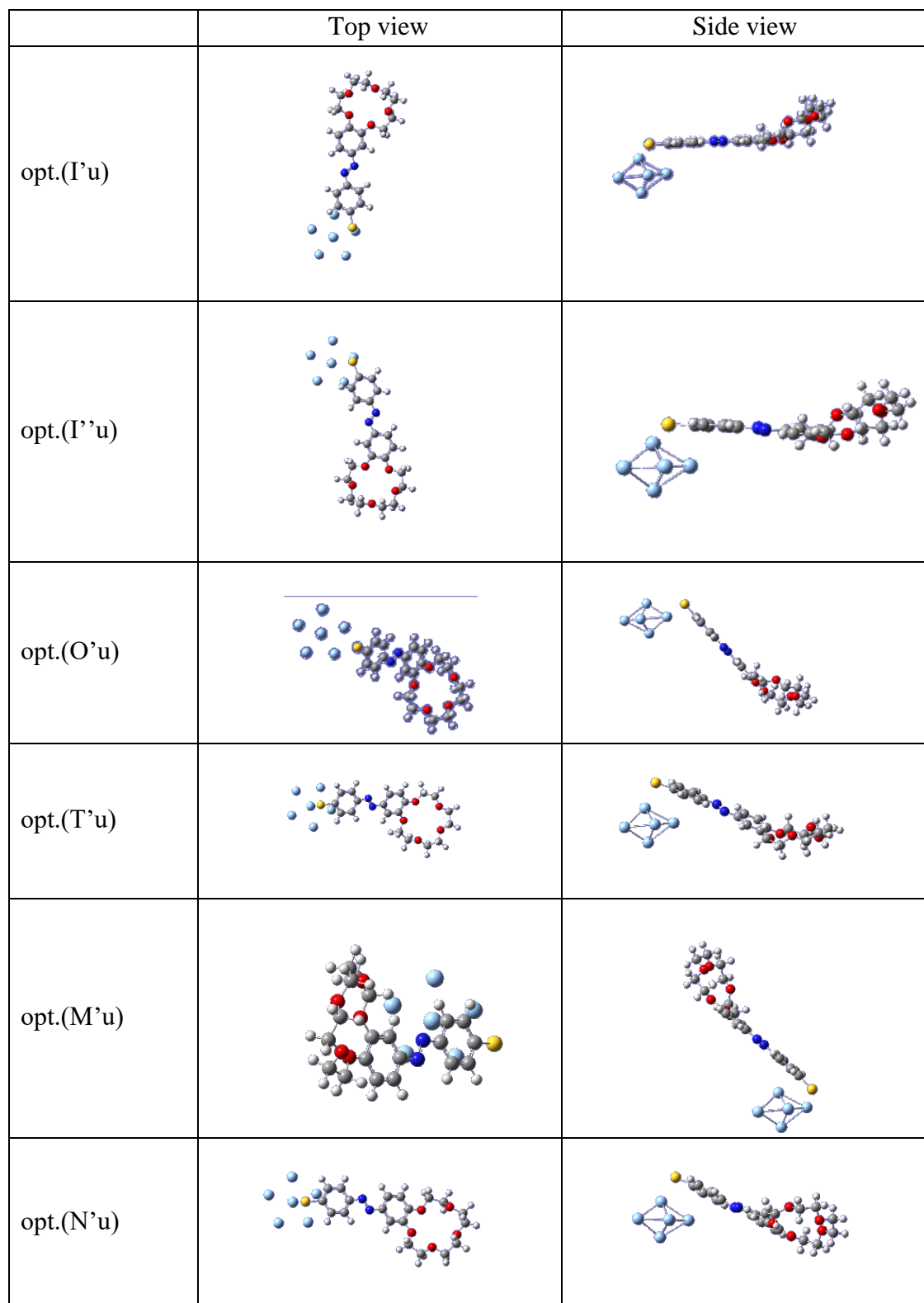


Figure S2. The side and top views of the six optimized structures of 4NB15C-4NTP-Ag₇ indicated, with the ether crown structure in the u-form.

Table S2 The indices for the relative orientation for 4NTP-4NB15C vs. Ag₇ with the ether crown d-form.

	opt.(I'd)	opt.(I''d)	opt.(O'd)	opt.(T'd)	opt.(M'd)	opt.(N'd)
S-Ag(A) (Å)	2.58	2.58	3.95	2.49	3.75	2.49
S-Ag(B) (Å)	3.66	4.18	2.68	4.21	2.73	3.91
S-Ag(C) (Å)	2.83	2.84	2.68	3.95	2.78	4.21
S-Ag(G) (Å)	4.89	4.90	4.76	5.41	4.86	5.39
∠Ag(A) – S – Ag(B)(°)	51.58	42.79	46.84	41.6	49.87	47.28
∠Ag(A) – S – Ag(C)(°)	64.34	64.17	46.86	46.61	49.75	41.59
∠Ag(A) – S – Ag(G)(°)	33.84	33.68	40.39	16.16	39.63	16.63
∠Ag(B) – S – Ag(C)(°)	50.35	42.97	64.50	40.85	62.39	40.98
α(°)	2.70	4.20	52.8	30.6	47.2	29.6
β(°)	35.5	37.9	14.6	26.5	24.8	30.6

Table S3. Indices for the relative orientations for 4NTP-4NB15C vs. Ag₇ with the ether crown u-form.

	opt.(I'u)	opt.(I''u)	opt.(O'u)	opt.(T'u)	opt.(M'u)	opt.(N'u)
S-Ag(A) (Å)	2.58	2.58	3.95	2.49	3.75	2.49
S-Ag(B) (Å)	3.66	4.18	2.68	4.22	2.73	3.91
S-Ag(C) (Å)	2.82	2.84	2.68	3.95	2.78	4.21
S-Ag(G) (Å)	4.89	4.90	4.76	5.40	4.86	5.39
∠Ag(A) – S – Ag(B)(°)	44.41	42.78	46.87	41.73	49.86	47.28
∠Ag(A) – S – Ag(C)(°)	64.31	64.13	46.90	46.85	49.75	41.55
∠Ag(A) – S – Ag(G)(°)	33.81	33.63	40.39	16.33	39.64	16.62
∠Ag(B) – S – Ag(C)(°)	50.30	43.01	64.52	40.85	62.41	40.97
α(°)	2.40	4.30	52.7	29.2	46.7	28.5
β(°)	35.8	37.9	14.4	30.5	22.1	29.3

2. Comparison of SERS spectra

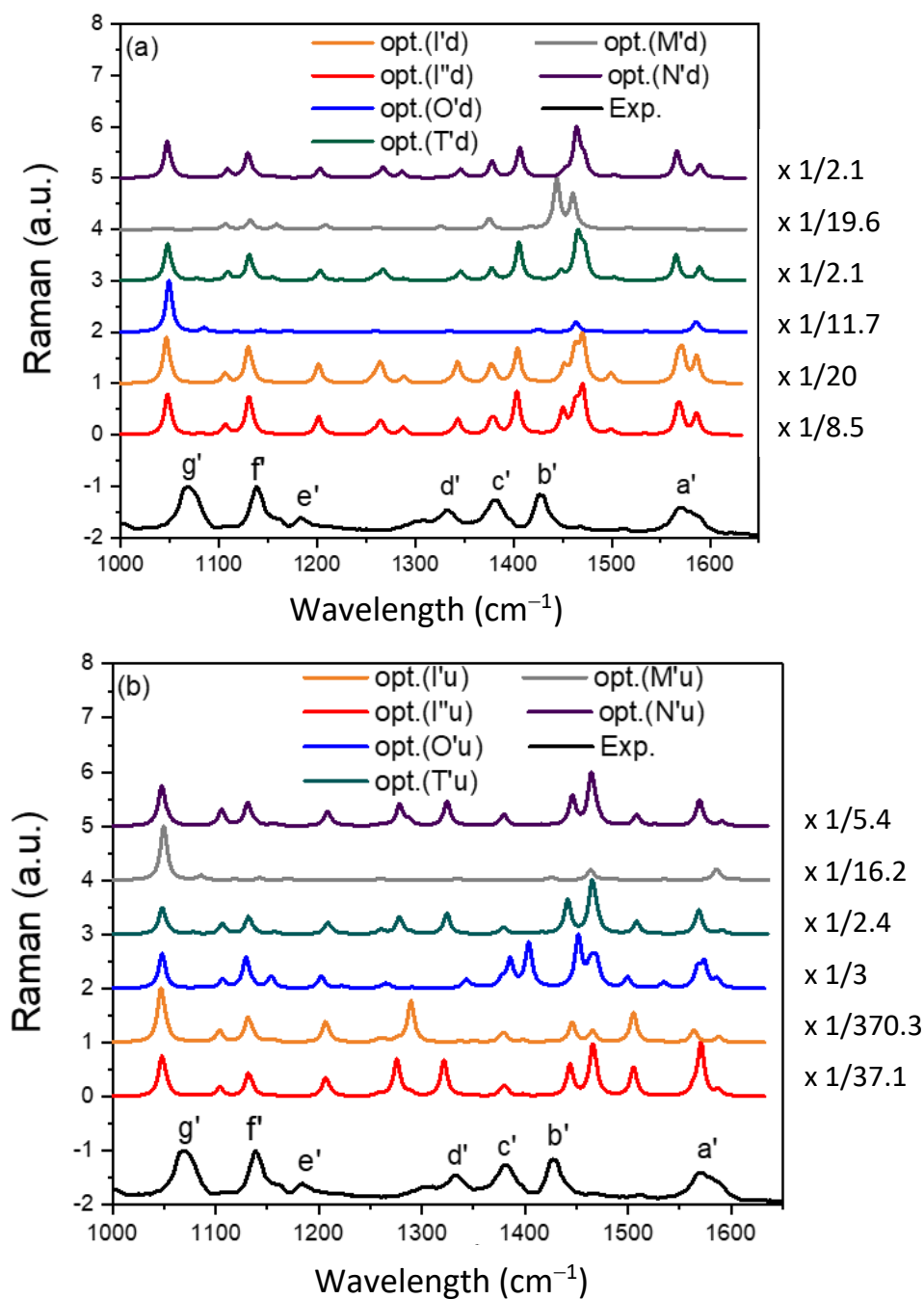


Figure S3. SERS simulations of 4NB15C-4NTP- Ag_7 by DFT calculations carried out at the B3LYP level, with the crown ether (a) d-form and (b) u-form (with species marked with *d* and *u* respectively). The simulated spectra are compared to that observed for the compound adsorbed on silver dendrite reported previously (Ref. 20 in text), on the basis of the labelled peaks a' - g' .

3. Comparison of the Raman spectra calculated with the PW91PW91 and B3LYP functional

We first optimized the adsorption structures of the 4NTP-Ag₇ by PW91PW91 with the pre-optimized Ag₇ structure fixed, following the same procedures done with the B3LYP functional. Two out of the six species obtained, labeled as I and O in Figure S4a, possess the Raman spectra that are consistent with the experimental data of 4NTP-AgDs. Their related orientations of 4-NTP to Ag₇ are about same as the opt.(I) and opt.(O) species obtained with the B3LYP functional. The quality of the calculated spectra with PW91PW91 is similar to that with B3LYP, which may be expected as there is no N=N coupling involved in the 4NTP-Ag₇. Each of the two optimized structures of the species I and O of 4NTP-Ag₇ generates two optimized *u* and *d* forms of 4NB15C-4NTP-Ag₇; these four conformations are labeled as PW91PW91-I'u, -O'u, -I'd, and -O'd, respectively. Figures S4b and S4c show the optimized structures and the corresponding Raman spectra (with a scaling factor 0.989) calculated with the PW91PW91 functional. From the calculated Raman spectra, ten vibrational modes (1-10), contributed mainly from the phenyl ring and the C-S stretching, are identified and correlated that from the B3LYP functional. The Raman modes labelled 1, 2, and 4-6 are assigned to N=N stretching vibrations, which correspond to the experimental band a', b' and c' in the Raman spectra of the Figures S4 b and c. Furthermore, we compare the respective deviations of the spectra calculated with the two functionals, with respect to the experimental data above 1300 cm⁻¹ (peaks 1-7). Similar deviations illustrated in Figure S5 suggest that the Raman spectra calculated with the two functionals PW91PW91 and B3LYP are of no obvious differences. Therefore, we conclude that in this particular case of 4NB15C-4NTP-Ag₇, the PW91PW91 and B3LYP functionals provide comparable results.

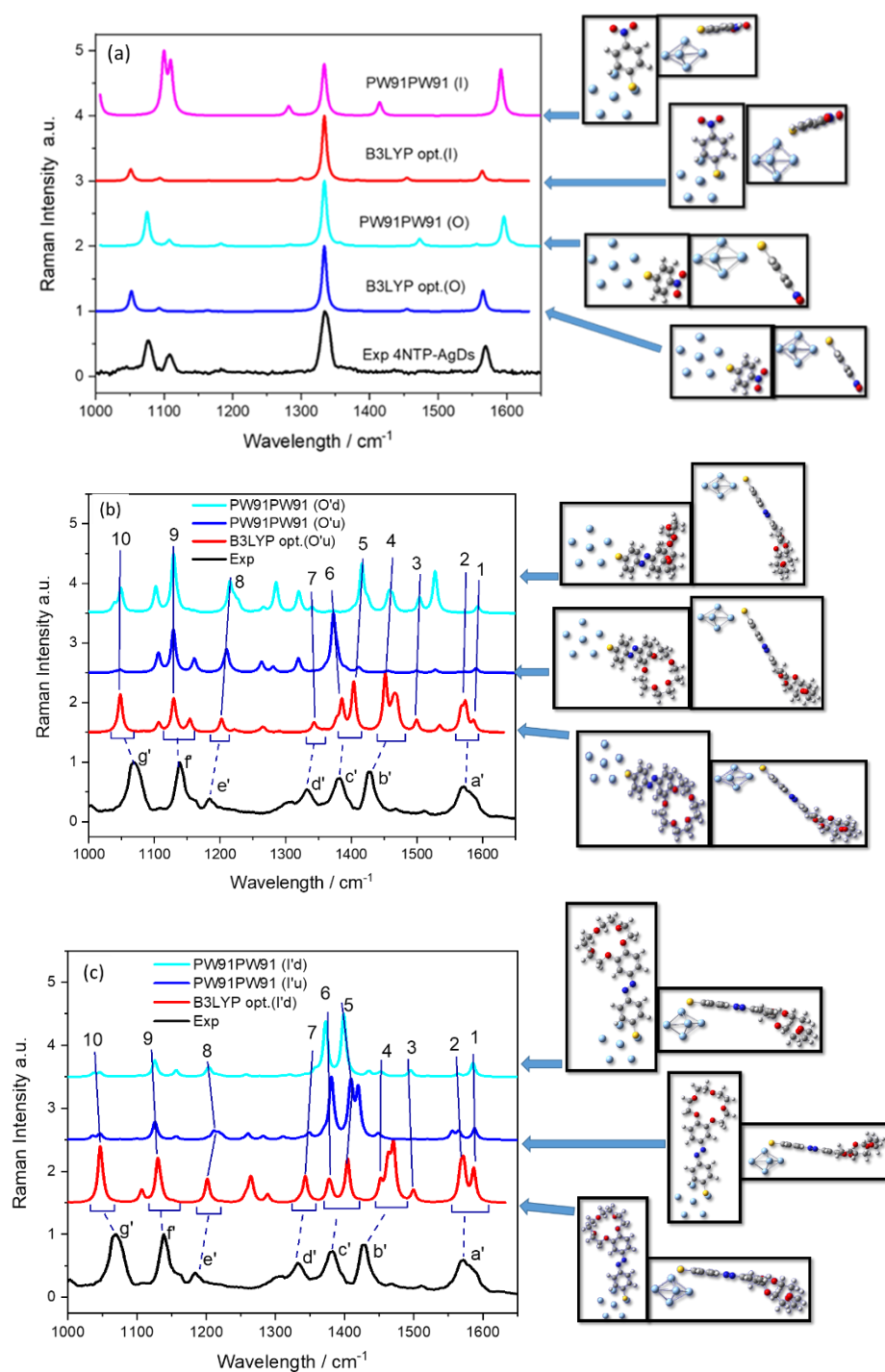


Figure S4. The comparison of relative orientations and Raman spectra calculated with the PW91PW91 [2,3] and B3LYP functionals for (a) the species O and I of 4NTP-Ag₇, (b) the species O' of 4NB15C-4NTP-Ag₇, and (c) the species I' of 4NB15C-4NTP-Ag₇. Ten vibrational modes (1-10) of opt.(O'u) are first assigned to the experimental results labelled a'-g'; then those peaks in the simulated Raman spectra are further associated with the solid and dashed lines.

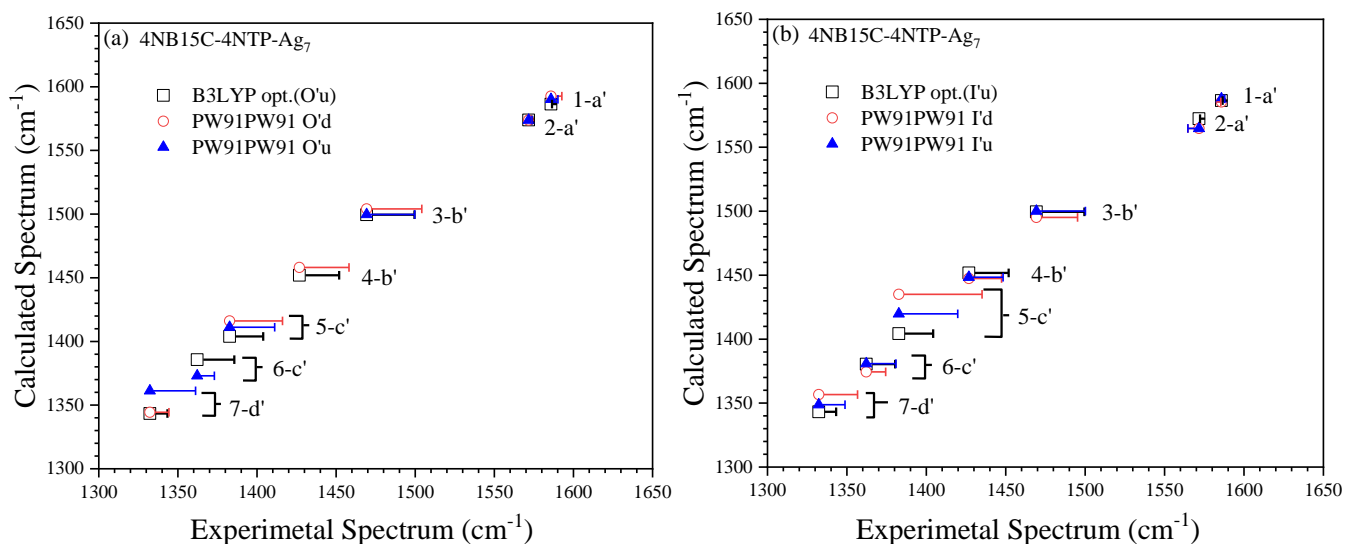


Figure S5. Calculated vibration spectra above 1300 cm⁻¹ with the (a) opt.O' and O' and (b) Opt.I' and I' species, using the functionals B3LYP (*u* form) and PW91PW91 (*d* and *u* forms) [1,2]. The calculated peaks (1-7) displayed along the *y*-axis are correlated to the experimental spectrum of band a' – d' displayed along the *x*-axis. Deviation quantities and directions of the calculated peaks, compared to the correlated experimental bands, are displayed by the horizontal bars (in black, red, and blue, with right- and left-hand-side for higher and lower frequency with respect to the measured band peaks). In general, the deviations of the calculated spectra from the two functionals are comparable.

4. Absorption spectrum of the Ag-dendrites used in the 4NB15C-4NTP SERS

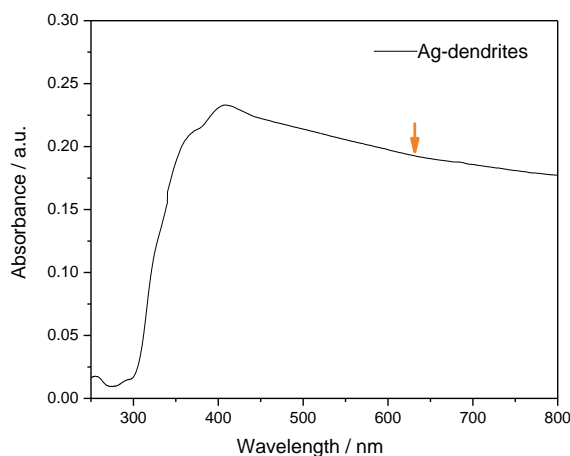


Figure S6. Absorption spectrum of the Ag-dendrites used in the 4NB15C-4NTP SERS measurements (cf. Ref. 20 in the text) using an integrating sphere device. The spectrum, not calibrated with possible re-absorption effect, exhibits absorption band covering 633 nm. [3]

5. TDDFT simulations at CAM-B3LYP level

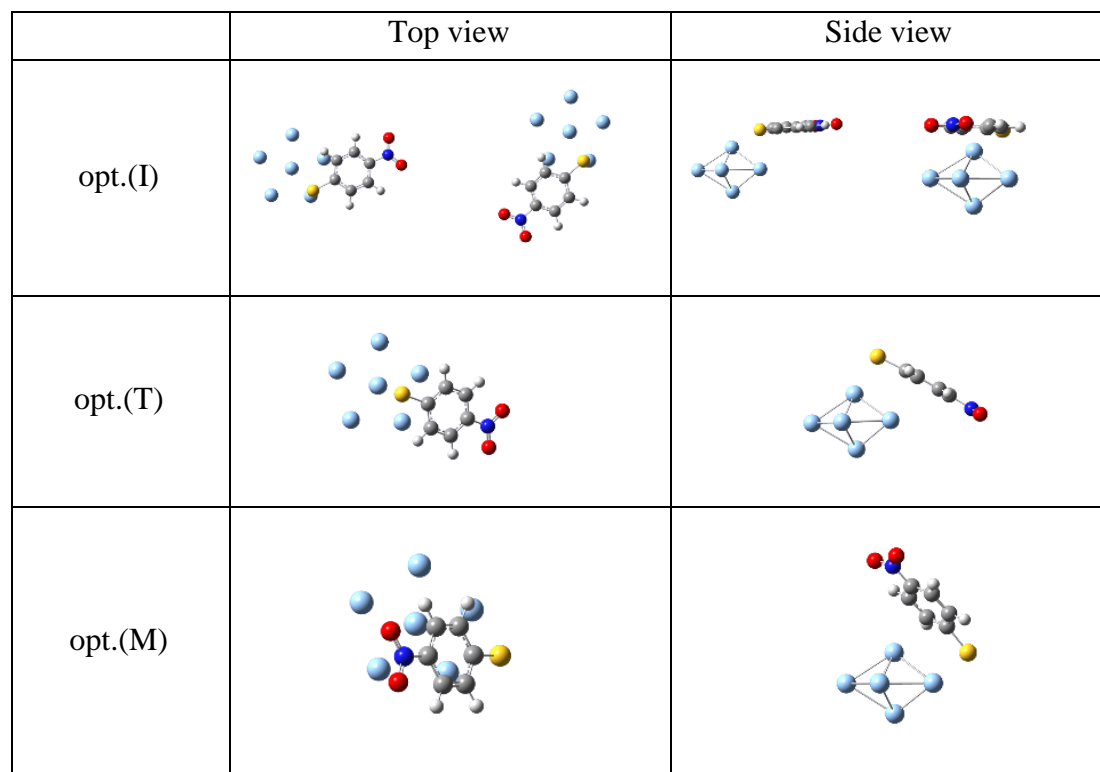


Figure S7. Side and top views of 4NTP-Ag₇ employed in TDDFT simulations at CAM-B3LYP level. Three optimized structures out of the thirteen initial structures are obtained, and labelled as opt.(I), opt.(T), and opt.(M). Mirror-symmetric structures, of identical SERS spectra, of opt.(I) are also shown.

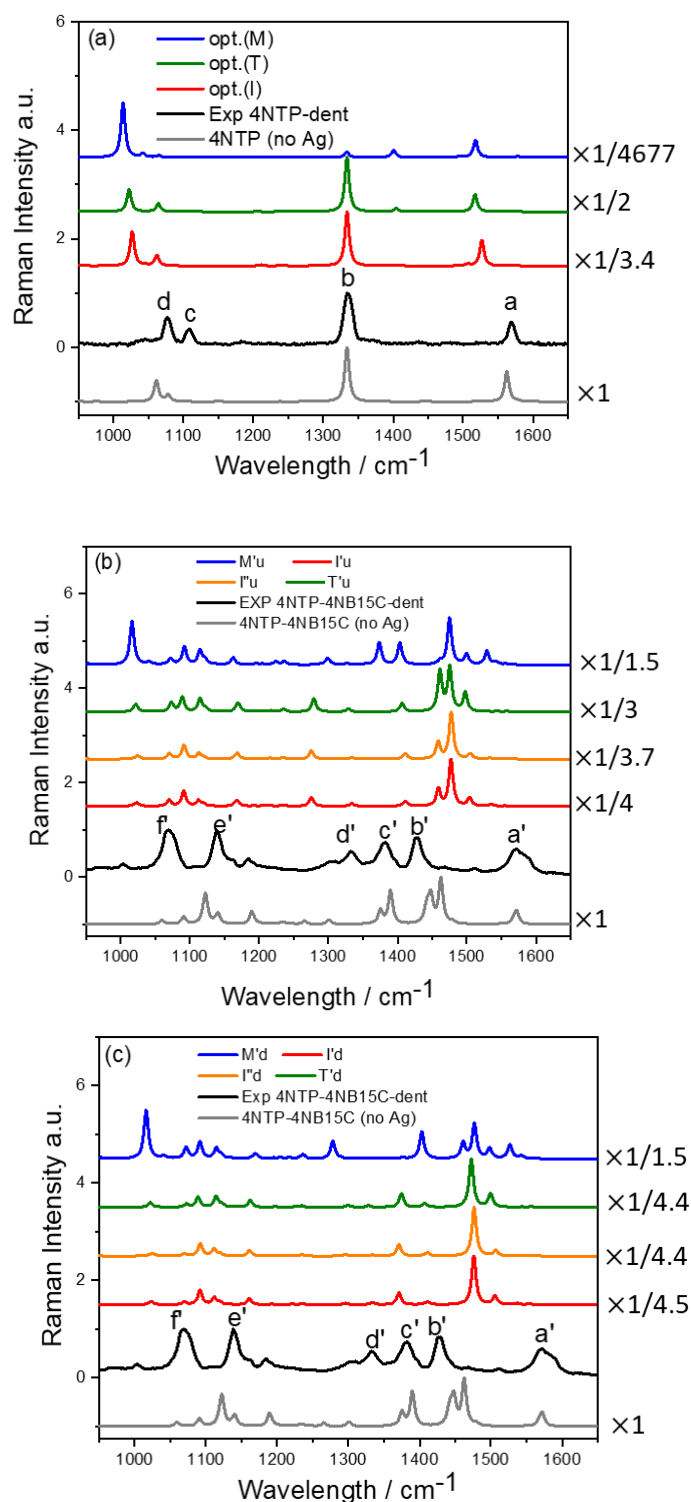


Figure S8. Calculated SERS spectra employed by TDDFT simulations at CAM-B3LYP level for (a) 4NTP-Ag₇ and the 4NTP without and with Ag₇, (b) 4NB15C-4NTP-Ag₇ with the crown ether u-form, and (c) SERS spectra of 4NB15C-4NTP-Ag₇ with the crown ether d-form, compared respectively to the measured SERS adsorbed compounds on silver dendrite surfaces. The calculated spectral intensities are rescaled by the ratios indicated (right-hand-side).

6. Peak-b assignment.

For a diatomic molecular motion, the vibrational amplitude ratio of atoms i and j is $d_i/d_j = m_j/m_i$, where m_i and d_i are the atomic weight and amplitude along the bonding. With the DFT calculation results of the peak-b in Fig. S8, the multi atomic coupled motion, the projections of the atomic displacements (N, C, and O) along the N-O and N-C bonds were considered respectively, as shown in Fig. S9. The projected amplitude ratio d_N/d_O along N-O bond is found ~ 0.8 , and d_N/d_C along N-C bond is ~ 3.7 . The d_N/d_O is close to the diatomic mass ratio compare to d_N/d_C . The results indicate the N-O stretching motional should dominate the vibrational motion of peak-b; therefore, the peak-b is assigned to N-O symmetric stretching mode.

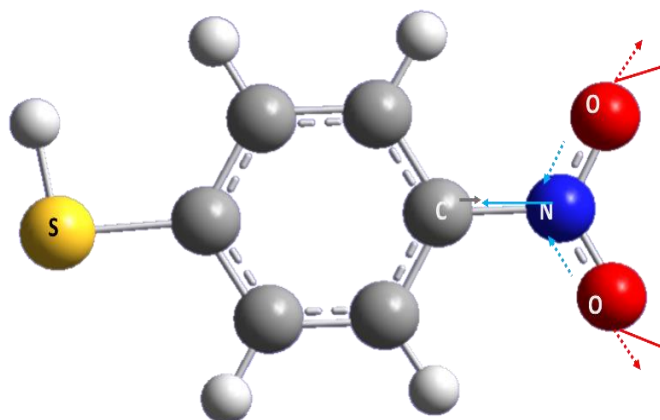


Figure S9. The solid arrows (gray, blue, and red) indicate the displacements direction of atoms C, N, and O, respectively. The blue and red dashed arrows indicate the vibration loci of atoms N and O along the N-O bond.

References:

- [1] D. Y. Wu, X. M. Liu, Y. F. Huang, B. Ren, X. Xu and Z. Q. Tian, *J. Phys. Chem. C*, 2009, 113, 18212-18222.
- [2] D.-Y. Wu, L.-B. Zhao, X.-M. Liu, R. Huang, Y.-F. Huang, B. Ren and Z.-Q. Tian, *Chem. Commun.*, 2011, 47, 2520-2522.
- [3] F. H. Cho, S. C. Kio, and Y. H. Lai, *RSC Adv.*, 2017, 7, 10259-10265.